Arabian Journal of Chemistry (2022) **15**, 104110

King Saud University

Arabian Journal of Chemistry

www.ksu.edu.sa
www.sciencedirect.com

ORIGINAL ARTICLE

Synthesis, bioactivity and preliminary mechanism of action of novel trifluoromethyl pyrimidine derivatives

Xuemei Tang [a,1], Wenliang Zhan [a,1], Shuai Chen [a], Ran Zhou [a], Die Hu [a], Nan Sun [a], Qiang Fei [b], Wenneng Wu [b,*], Wei Xue [a,*]

[a] *State Key Laboratory Breeding Base of Green Pesticide and Agricultural Bioengineering, Key Laboratory of Green Pesticide and Agricultural Bioengineering, Ministry of Education, Research and Development Center for Fine Chemicals, Guizhou University, Guiyang 550025, PR China*
[b] *Food and Pharmaceutical Engineering Institute, Guiyang University, Guiyang 550003, PR China*

Received 6 June 2022; accepted 4 July 2022
Available online 9 July 2022

KEYWORDS

Trifluoromethyl pyrimidine;
Antiviral activity;
Antifungal activity;
Mechanism of action

Abstract In this study, a series of trifluoromethyl pyrimidine derivatives **5a-5v** were designed and synthesized. All synthetic compounds were original. Bioassay results showed that some of the target compounds were proved to have higher antiviral and antifungal activities than those of commercial agents. Especially, EC_{50} values of the curative activity of compound **5j** and the protection activity of compound **5m** were 126.4 and 103.4 μg/mL, respectively, which were lower than that of ningnanmycin. Microscale thermophoresis experiment proved that there was a good interaction between compound **5m** and TMV-CP. Meanwhile, the antifungal activity results showed that compound **5u** had a significant on *in vitro* against *Rhizoctonia solani* (*RS*) activity, with the EC_{50} value of 26.0 μg/mL, which was equal to that of azoxystrobin. As well, *in vivo* experiments on rice leaves

Abbreviations: ^{1}H NMR, ^{1}H nuclear magnetic resonance; ^{13}C NMR, ^{13}C nuclear magnetic resonance; ^{19}F NMR, ^{19}F nuclear magnetic resonance; HRMS, High-resolution mass spectrometry; EC_{50}, Median effective concentration; TMV, Tobacco mosaic virus; AB, Alternaria brassicae; FF, Fusarium fujikuroi; FO, Fusarium oxysporum f.sp.cucumerinum; CT, Colletotrichum truncatum; PC, Phytophthora capsici; CG, Colletotrichum gloeosporioides; RS, Rhizoctonia solani; FG, Fusarium graminearum; PS, Phytophthora sojae; PP, Phytophthora palmivora; BC, Botrytis cinerea; PL, Phytophthora litchii

[1] These authors contributed equally to this work.

* Corresponding authors.
E-mail addresses: wuwenneng123@126.com (W. Wu), wxue@gzu.edu.cn (W. Xue).

Peer review under responsibility of King Saud University.

Production and hosting by Elsevier

https://doi.org/10.1016/j.arabjc.2022.104110

showed that compound **5u** could effectively control *RS*, and the effect of **5u** on the cell morphology of *RS* was observed by scanning electron microscopy.

1. Introduction

Food is the basic need of mankind to maintain the health and survival, as well as an important strategic material that affects national security, political security and economic development (Hao et al., 2020). In our daily life, grains, vegetables, and fruits are important components of human food (Chen et al., 2018). However, plant diseases caused by bacteria, fungi, and viruses are extremely difficult to control in agricultural production, seriously affecting the yields and quality of crops and causing huge economic losses (Ji et al., 2016; Lu et al., 2014). Chemical agents are one of the important ways to protect crop products. Long-term use and irregular use inevitably lead to increasing drug resistance and prominent ecological risks (Zhang et al., 2019). Therefore, it is of great significance to develop new pesticides with new structures and high activity (Jiang et al., 2020).

Pyrimidine is an important part of *N*-containing heterocyclic compound that were widely distributed in the nature, such as caffeine, vitamin B, theophylline, and so on (Liu et al., 2021a,b). Meanwhile, due to its extensive pesticide biological activities, such as anticancer (Wang et al., 2021; Munikrishnappa et al., 2021; Alia et al., 2021; Sankarganesha et al., 2021; Zühal et al., 2020), anti-inflammatory (Purushothaman et al., 2018), antimalarial (Mane et al., 2014), anti-leukemia (Yang et al., 2013), antitumor (Liu et al., 2021a,b; Guo et al., 2020a,b), immunomodulatory (Dolsak et al., 2021), insecticide (Wu et al., 2019a,b; Chen et al., 2013), herbicidal (Zuo et al., 2016), antiviral (Zan et al., 2020; Mamdouh et al., 2021; Alaa et al., 2022) and antifungal (Zhang et al., 2016; Mohammareh et al., 2020; Chen et al., 2022; Samata et al., 2022) activity, etc (Wang et al., 2017; Seenaiah et al., 2014; Emami et al., 2020), pyrimidine was found to be one of the most important active fragments in pesticide chemistry and some commercialized pyrimidine pesticides (Fig. 1) have been successfully developed. The reason for introducing phenyl ether and ester moieties into the molecular skeleton, on the one hand, because these groups are found in many commercial drugs, and on the other hand, the introduction of these groups can increase the water solubility of compounds. In our previous work, we also found that pyrimidine derivatives revealed good antifungal (Wu et al., 2021), antiviral (Wu et al., 2015), insecticidal (Wu et al., 2020), and antibacterial activities (Su et al., 2021).

In this study, considering that pyrimidine compounds had a wide range of biological activities, we obtained a series of trifluoromethyl pyrimidine derivatives through ring closure, chlorination, substitution and other reactions from ethyl trifluoroacetoacetate. The target compounds were screened for antiviral and antifungal activity. Subsequently, Microscale thermophoresis (MST) and molecular docking experiments were performed on compound **5m** with excellent antiviral activity to further confirm its application prospects in the development of antiviral agents. In addition, *in vivo* experiment of **5u** against *Rhizoctonia solani* (*RS*) was carried out and the effects of **5u** on *RS* cells was observed and evaluated by scanning electron microscopy. The antifungal action mechanism of the target compound **5u** was preliminarily discussed.

2. Materials and methods

2.1. Instruments and chemicals

The melting points were determined by using an XT-4 binocular microscope (Beijing Tech. Instrument Co., China) and uncorrected. Proton nuclear magnetic resonance ^{1}H NMR, ^{13}C NMR, and ^{19}F NMR spectra were obtained by using an ASCEND 400 NMR (Bruker Optics, Switzerland) spectrometer operated at room temperature with $CDCl_3$ as the solvent and tetramethylsilane as the internal standard. High-resolution mass spectrometry (HRMS) was conducted by using a Thermo Scientific Q Exactive (Thermo Scientific, Missouri, USA). The X-ray crystal data were obtained by Bruker D8-QUEST diffractometer (Bruker Optics, Switzerland). The chemical materials and reagents were purchased from commercial suppliers and all reagents are analytical pure solvents made in China.

2.2. Synthesis

*General Procedures for Preparing Intermediates **1–4** and the Compounds **5a–5v***. A series of trifluoromethyl pyrimidine derivatives (**5a-5v**) were designed and synthesized according to Scheme 1. Intermediates **1, 2, 3,** and **4** were synthesized by the reported methods (Wu et al., 2019a,b; Yu et al., 2021). The intermediate **4**, halohydrocarbon and K_2CO_3 were reacted in DMF for 6–8 h at ice-bath. TLC was used to monitor the reaction. The crude product was purified by column chromatography (*V*/*V*, petroleum ether: ethyl acetate = 15:1 to 8:1) to obtain the compounds **5a-5v**. The specific preparation methods of the target compounds **5a-5v** were provided in Supporting Information.

2.3. Antiviral bioactivity

The anti-TMV activities assay of target compounds according to the method had reported (Luo et al., 2020; Chen et al., 2020). The microscale thermophoresis and molecular docking have been performed using our previously reported methods (Guo et al., 2020a,b; Tang et al., 2019). Common leaf K326 (Nicotiana Tabacum K326), extracted from tobacco Mosaic virus; Nicotiana glutinosa, the host of TMV.

2.4. Antifungal bioactivity

The *in vitro* and *in vivo* antifungal assay, sclerotia germination inhibition sclerotia formation inhibition tests and scanning electron microscopy experiments were performed according to the literature methods reported (Wang et al., 2019; Zhang et al., 2018a,b; Shi et al., 2020; Zhang et al., 2018a,b).

3. Results and discussion

3.1. Chemistry

As shown in Scheme 1, compounds **5a-5v** were synthesized, and characterized their structures by ^{1}H NMR, ^{13}C NMR, ^{19}F NMR and HRMS. All synthetic compounds were original.

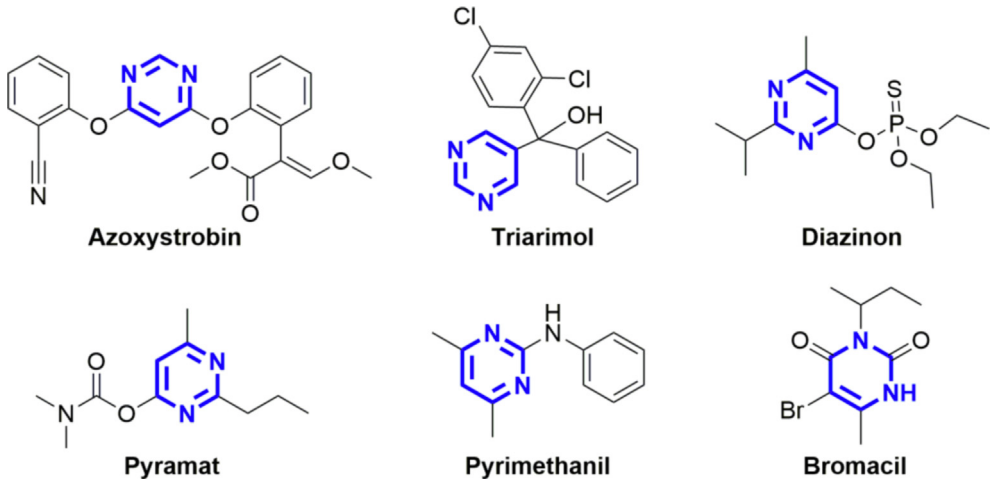

Fig. 1 The structures of some commercialized pyrimidine pesticides.

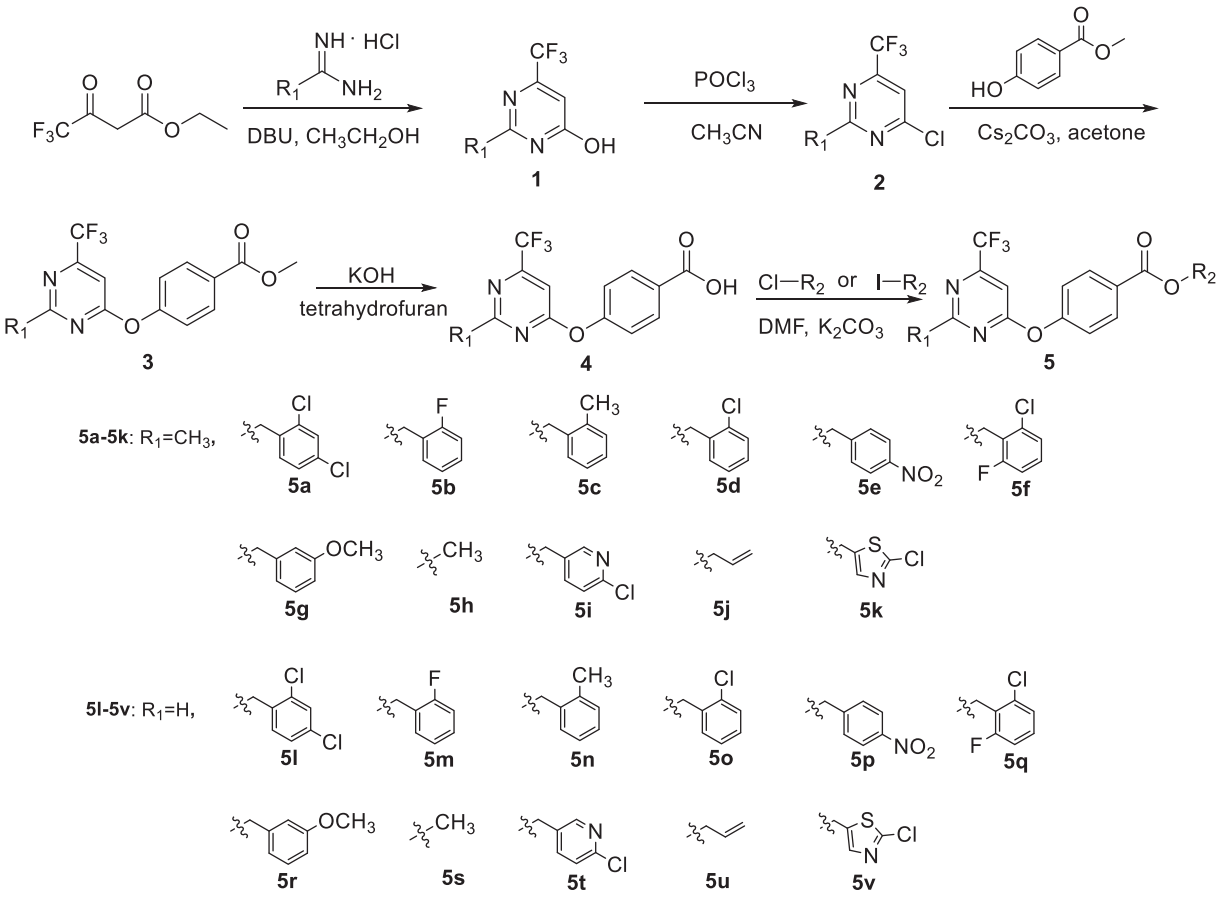

Scheme 1 Synthetic route of the target compounds **5a-5v.**

The specific data were displayed in the Supporting Information.

Meanwhile in order to further determine the structure of the target compounds, compounds **5d** and **5f** were successfully cultured into a single crystal and analyzed their structures by single crystal X-ray diffraction. The crystal structures of **5d** (deposition CCDC 2121760) and **5f** (deposition CCDC 2121761) were shown in Fig. 2. More characterization data were supplied in the Supporting Information.

3.2. Antiviral assay

*3.2.1. Antiviral activity of compounds **5a-5v** against TMV in vivo*

The half-leaf spot method was used to evaluate the antiviral activity of the target compounds against TMV *in vivo* at 500 μg/mL. Table 1 showed that the target compounds **5a-5v** exhibited moderate to good anti-TMV activity, with the cura-

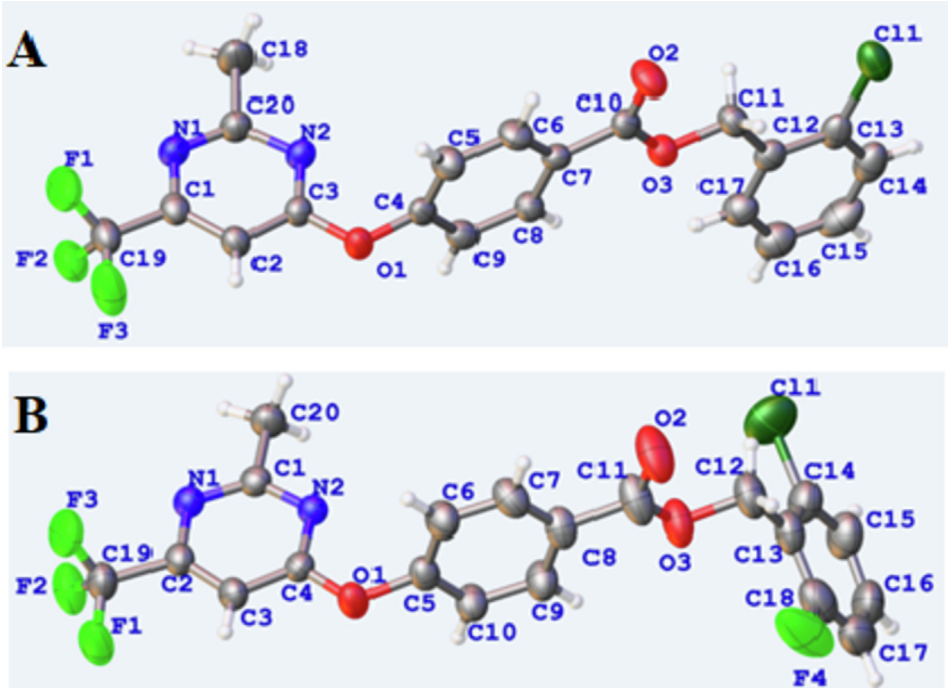

Fig. 2 The crystal X-ray structures of compounds **5d** (A) and **5f** (B).

Table 1 Antiviral activity of target compounds against TMV *in vivo* at 500 μg/mL.

Compounds	Curative activity (%)[a]	Protection activity (%)[a]	Inactivated activity (%)[a]
5a	59.8 ± 0.1	58.1 ± 0.2	49.6 ± 0.1
5b	70.1 ± 5.2	42.1 ± 3.7	41.4 ± 0.2
5c	44.4 ± 0.3	42.9 ± 4.5	45.1 ± 0.4
5d	32.8 ± 0.1	45.6 ± 2.5	56.1 ± 0.2
5e	48.2 ± 0.1	35.2 ± 0.1	76.7 ± 0.1
5f	55.6 ± 0.7	65.7 ± 0.2	56.9 ± 0.2
5g	49.1 ± 0.1	56.9 ± 5.0	45.2 ± 0.1
5h	38.0 ± 5.2	66.4 ± 0.2	51.5 ± 0.1
5i	39.3 ± 6.1	42.2 ± 3.8	64.1 ± 0.1
5j	76.3 ± 0.1	49.1 ± 1.5	51.4 ± 0.2
5k	56.0 ± 0.6	62.1 ± 0.8	23.2 ± 1.2
5l	64.1 ± 0.6	32.9 ± 0.5	64.0 ± 0.2
5m	66.1 ± 0.7	65.5 ± 0.3	56.4 ± 0.1
5n	48.7 ± 0.1	37.1 ± 0.6	46.5 ± 0.1
5o	42.7 ± 0.1	38.8 ± 2.5	46.1 ± 0.2
5p	54.4 ± 3.0	55.8 ± 1.0	57.5 ± 0.1
5q	71.3 ± 0.1	62.7 ± 1.0	51.1 ± 4.9
5r	32.4 ± 0.1	47.7 ± 0.1	69.3 ± 2.9
5s	64.2 ± 0.6	61.6 ± 0.1	69.3 ± 1.0
5t	53.1 ± 0.1	23.9 ± 0.9	66.9 ± 2.8
5u	41.1 ± 1.4	60.4 ± 0.7	39.7 ± 2.4
5v	50.8 ± 1.2	26.2 ± 2.5	60.6 ± 0.2
Ningnanmycin[b]	54.0 ± 0.2	58.6 ± 0.7	94.9 ± 0.1

[a] Average of three replicates.
[b] The commercial antiviral agent.

tive, protection, and inactivation activity ranges of 32.4–76.3%, 23.9–66.4%, and 23.2–76.7%, respectively. Among of them, compounds **5b**, **5j**, **5l**, **5m**, **5q**, and **5s** had significant curative activity against TMV, with the inhibition rates of 70.1, 76.3, 64.1, 66.1, 71.3 and 64.2%, respectively, which were better than that of ningnanmycin (54.0%). Meanwhile, compounds **5f**, **5h**, **5m**, **5q**, and **5s** showed remarkable protection activity against TMV, with the inhibition rates of 65.7, 66.4, 65.5, 62.7 and 61.6%, respectively, which were superior to ningnanmycin (58.6%). In vivo leaf diagram of compound **5m** was shown in Fig. 3.

EC_{50} values of some target compounds were further evaluated and the test results were listed in Table 2. Table 2 showed that the tested compounds **5b**, **5f**, **5h**, **5j**, **5k**, **5l**, **5m**, **5q** and **5s** revealed better curative or protective activity, and EC_{50} values were better than those of ningnanmycin. Among of them, com-

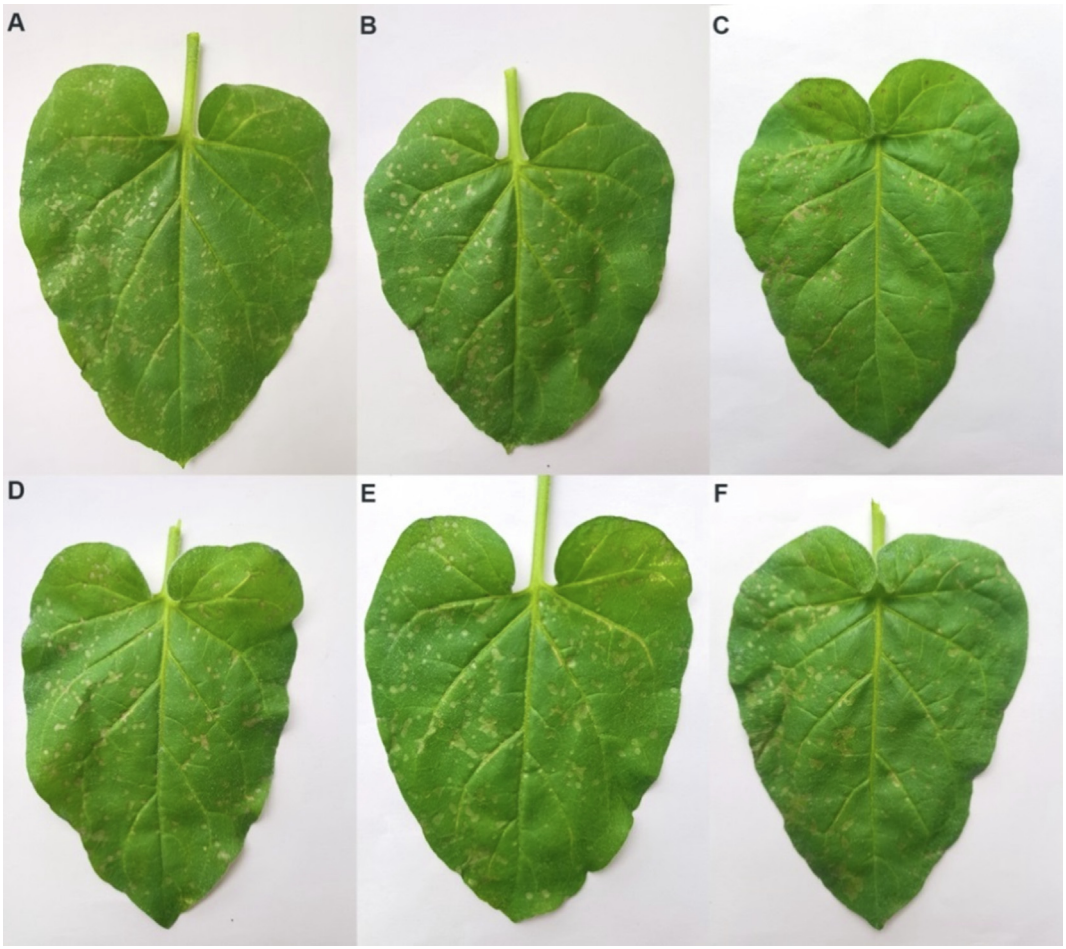

Fig. 3 Anti-TMV activities of **5m** (A. Curative activity, B. Protection activity, C. Inactivated activity) and ningnanmycin (D. Curative activity, E. Protection activity, F. Inactivated activity) *in vivo*.

Table 2 EC_{50} values of some of the target compounds against TMV *in vivo*.

Compounds	EC_{50} (μg/mL)[a]	
	Curative activity	Protection activity
5b	205.4	–
5f	–	122.1
5h	–	111.6
5j	126.4	–
5k	–	191.8
5l	257.8	–
5m	169.1	103.4
5q	139.3	191.2
5s	174.9	–
Ningnanmycin[b]	362.7	255.1

[a] Average of three replicates.
[b] The commercial antiviral agent.

pound **5j** has the best curative activity, with EC_{50} value of 126.4 μg/mL, which was better than that of ningnanmycin (362.7 μg/mL). Compound **5m** showed significant protective activity with EC_{50} value of 103.4 μg/mL, which was superior to that of ningnanmycin (255.1 μg/mL).

The structure–activity relationship (SAR) analyzed on the basis of the antiviral activities against TMV shown in Table 1. When R_1 and R_2 was CH_3 group, the target compound had the best protective activity against TMV. For example, the protective activities of compounds **5h** (R_1 = CH_3, R_2 = CH_3), **5f** (R_1 = CH_3, R_2 = 2-Cl-6-F-Ph) and **5k** (R_1 = CH_3, R_2 = 2-Cl-5-thiazoly) were 66.4, 65.7 and 62.1%, respectively, which were superior to other substituents. In addition, when R_1 was H, the protective activities of compounds **5m** (R_1 = H, R_2 = 2-F-Ph), **5q** (R_1 = H, R_2 = 2-Cl-6-F-Ph), **5s** (R_1 = H, R_2 = CH_3) and **5v** (R_1 = H, R_2 = 2-Cl-5-thiazoly) were 65.5, 62.7, 61.6 and 60.4%, respectively. In terms of the curative activity data of the target compounds against TMV, compounds **5j** (76.3%) > **5q** (71.3%) > **5b** (70.1%) > **5m** (66.1%) > **5s** (64.2%) > **5l** (64.1%), in which compounds **5b** (R_1 = CH_3, R_2 = 2-F-Ph) and **5m** (R_1 = H, R_2 = 2-F-Ph) had different R_1 groups and same R_2 groups. It is speculated that when 2-F-Ph at the R_2 position, R_1 was electron donor group which could enhance the protective and curative activities of the target compounds against TMV at 500 μg/mL. It can be seen from the test results of anti-TMV activity in Table 1 that compound **5s** (R_1 = H, R_2 = CH_3) has excellent anti-TMV activity in terms of protective, curative and inactivated activities compared with com-

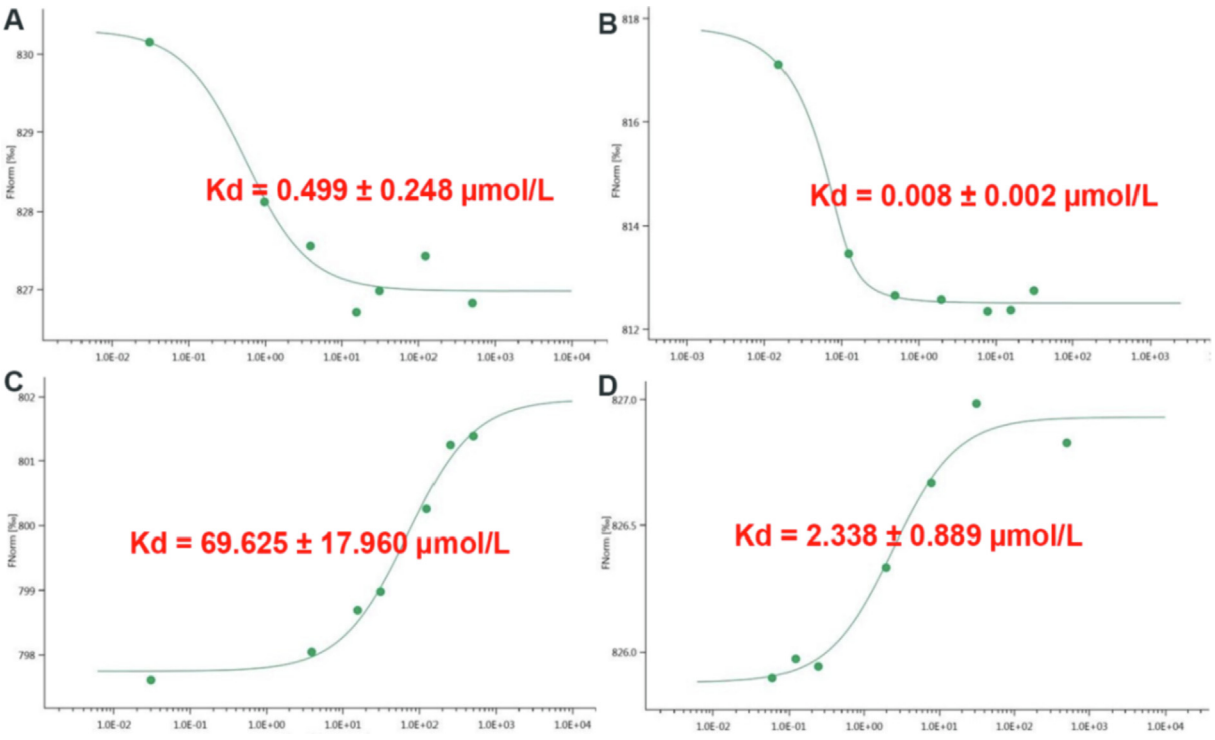

Fig. 4 MST results of compounds **5h** (A), **5m** (B), **5t** (C) and ningnanmycin(D).

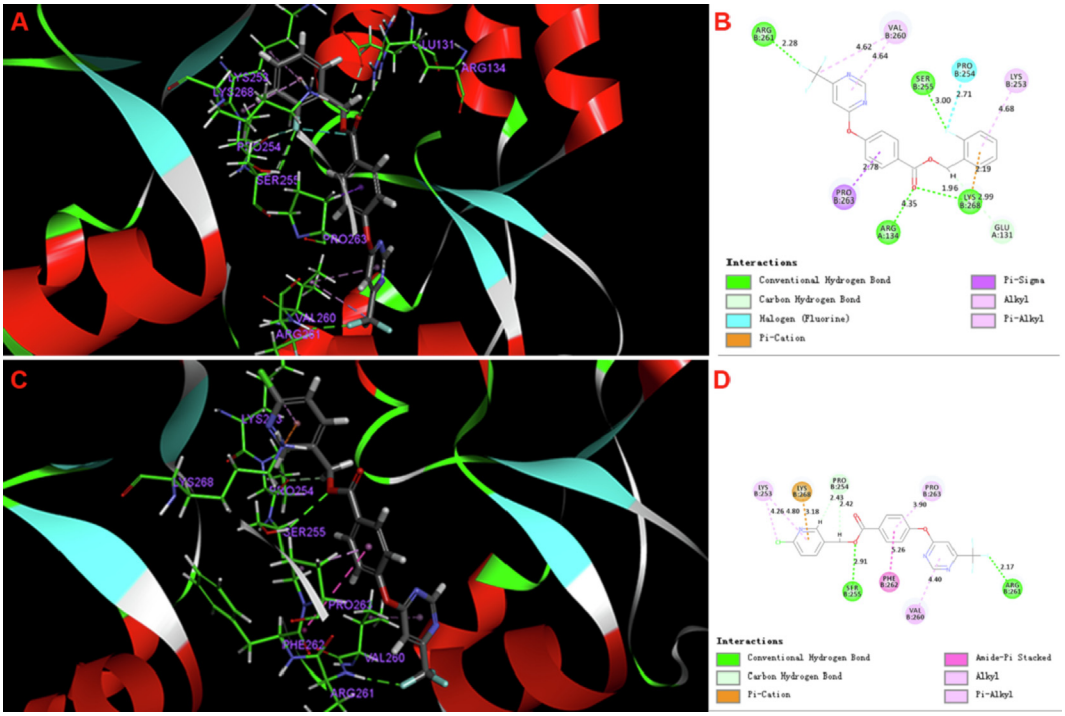

Fig. 5 Molecular docking results of compounds **5m** (A and B), **5t** (C and D).

pounds **5h** (R_1 = CH_3, R_2 = CH_3) and **5o** (R_1 = H, R_2 = 2-Cl-Ph) of the same series. Indicating that the introduction of a CH_3 group at the R_2 position could improve the biological activity of the compound under the condition that the H atom at the 2-position of the pyrimidine remains unchanged.

*3.2.2. Binding sites of **5h**, **5m**, **5t** and ningnanmycin to TMV-CP*

Microscale thermophoresis (MST) was used to further analyze the interaction of compounds **5h**, **5m**, **5t** and ningnanmycin with tobacco mosaic virus coat protein (TMV-CP). The MST results were shown in Fig. 4, where the binding of

Table 3 *In vitro* antifungal activity of the target compounds against the testing fungi.

Compounds	Inhibition rate (%)[a]											
	AB	*FF*	*FO*	*CT*	*PC*	*CG*	*RS*	*FG*	*PS*	*PP*	*BC*	*PL*
5a	25.0 ± 4.3	18.3 ± 1.1	7.8 ± 1.3	12.7 ± 0.3	21.9 ± 2.2	25.8 ± 1.6	38.6 ± 2.8	19.7 ± 1.6	32.8 ± 1.9	11.8 ± 2.3	36.1 ± 0.1	–
5b	17.5 ± 1.9	13.4 ± 2.8	6.5 ± 2.3	25.0 ± 0.2	21.4 ± 2.8	42.5 ± 1.6	65.3 ± 1.7	14.0 ± 3.2	33.7 ± 0.6	25.4 ± 2.3	25.0 ± 2.7	76.3 ± 3.1
5c	18.8 ± 1.7	29.8 ± 2.1	6.5 ± 1.8	19.7 ± 0.5	17.9 ± 3.0	22.3 ± 3.5	41.6 ± 2.3	21.9 ± 1.0	28.5 ± 1.7	8.7 ± 1.8	19.0 ± 0.5	20.1 ± 3.9
5d	5.2 ± 2.8	17.2 ± 2.8	5.2 ± 1.1	5.2 ± 0.1	5.2 ± 2.8	5.2 ± 1.7	5.2 ± 3.1	5.2 ± 0.8	5.2 ± 4.2	5.2 ± 0.1	24.3 ± 4.4	5.2 ± 1.4
5e	28.0 ± 1.9	36.7 ± 2.8	9.2 ± 3.0	17.1 ± 0.4	7.4 ± 1.5	18.8 ± 0.8	17.5 ± 1.9	25.0 ± 1.7	24.1 ± 3.7	16.6 ± 2.2	18.0 ± 3.6	18.8 ± 3.1
5f	22.3 ± 2.4	27.5 ± 3.8	3.5 ± 1.1	21.0 ± 0.1	10.0 ± 1.6	26.3 ± 1.9	41.2 ± 4.6	21.9 ± 2.2	25.4 ± 2.4	12.7 ± 2.6	37.2 ± 1.4	17.5 ± 2.8
5g	20.1 ± 2.8	12.2 ± 3.3	1.7 ± 2.6	23.6 ± 0.3	22.8 ± 2.9	24.1 ± 2.1	45.6 ± 1.9	13.6 ± 1.6	28.5 ± 4.0	16.6 ± 3.6	24.4 ± 2.3	77.3 ± 0.1
5h	32.0 ± 0.7	22.9 ± 1.2	3.9 ± 1.2	17.9 ± 0.2	29.8 ± 3.6	23.6 ± 2.3	63.1 ± 1.4	19.3 ± 2.9	21.0 ± 0.1	23.2 ± 1.6	31.0 ± 0.3	77.3 ± 0.2
5i	24.1 ± 0.9	29.8 ± 2.8	7.4 ± 2.1	73.2 ± 0.2	19.3 ± 4.1	49.1 ± 2.2	64.4 ± 2.8	6.5 ± 1.0	26.7 ± 4.0	35.0 ± 1.1	16.3 ± 3.6	81.5 ± 2.1
5j	43.8 ± 4.3	32.5 ± 2.1	12.2 ± 2.2	63.1 ± 0.1	36.4 ± 3.9	45.6 ± 2.9	67.5 ± 2.1	24.5 ± 0.8	23.2 ± 3.4	15.7 ± 3.7	19.8 ± 1.8	40.7 ± 1.1
5k	30.2 ± 4.3	29.1 ± 2.7	3.5 ± 1.1	48.6 ± 0.3	17.1 ± 1.5	62.2 ± 1.1	68.8 ± 4.1	12.2 ± 2.2	25.1 ± 4.3	31.8 ± 0.2	25.5 ± 0.9	90.1 ± 4.3
5l	19.7 ± 2.4	19.1 ± 4.9	20.6 ± 2.5	28.5 ± 0.3	21.4 ± 2.8	27.1 ± 1.9	39.4 ± 2.1	–	32.4 ± 4.1	22.8 ± 4.1	28.1 ± 3.3	38.1 ± 2.7
5m	17.1 ± 4.3	28.7 ± 4.8	22.8 ± 4.3	25.8 ± 0.3	17.1 ± 2.3	37.7 ± 1.1	56.5 ± 3.8	22.8 ± 1.6	22.3 ± 3.2	45.1 ± 2.6	34.2 ± 0.5	51.7 ± 1.7
5n	19.3 ± 2.4	29.1 ± 1.4	21.4 ± 3.2	26.7 ± 0.2	27.1 ± 0.2	32.8 ± 1.0	49.5 ± 1.7	34.2 ± 0.1	27.1 ± 3.5	13.6 ± 1.6	24.7 ± 1.1	55.2 ± 2.7
5o	18.4 ± 3.3	24.5 ± 2.4	23.2 ± 2.0	24.1 ± 0.2	14.0 ± 1.8	27.6 ± 1.7	48.2 ± 1.9	12.2 ± 1.6	14.9 ± 2.8	28.5 ± 0.9	33.2 ± 2.2	75.8 ± 1.5
5p	12.2 ± 1.9	29.1 ± 3.0	18.8 ± 1.4	11.4 ± 0.3	7.4 ± 1.5	22.3 ± 1.6	41.2 ± 1.2	–	27.1 ± 5.4	21.0 ± 3.1	35.4 ± 4.8	87.3 ± 0.1
5q	20.1 ± 1.2	14.9 ± 4.6	17.1 ± 4.1	34.6 ± 0.2	21.0 ± 2.5	27.1 ± 1.1	48.6 ± 1.2	6.5 ± 1.7	–	16.6 ± 1.1	17.0 ± 0.9	93.8 ± 0.2
5r	22.8 ± 2.4	26.4 ± 2.9	18.4 ± 1.9	30.2 ± 0.7	27.1 ± 3.5	32.0 ± 3.1	41.2 ± 1.2	22.3 ± 1.7	20.6 ± 4.0	25.4 ± 4.6	34.4 ± 4.2	48.6 ± 3.4
5s	25.8 ± 1.7	46.3 ± 1.0	28.9 ± 1.3	17.1 ± 0.1	40.7 ± 1.4	30.2 ± 4.0	67.3 ± 0.2	52.6 ± 5.0	34.2 ± 0.2	64.9 ± 1.1	19.8 ± 2.8	96.3 ± 1.2
5t	34.6 ± 1.7	29.8 ± 3.6	19.7 ± 2.3	71.0 ± 0.2	31.1 ± 3.6	56.5 ± 1.1	71.9 ± 1.2	21.0 ± 0.8	21.0 ± 3.2	45.1 ± 1.6	22.1 ± 1.8	96.0 ± 1.7
5u	65.7 ± 2.0	42.1 ± 1.5	25.0 ± 1.8	55.2 ± 0.4	49.1 ± 4.2	60.0 ± 3.7	88.6 ± 1.2	46.0 ± 2.2	–	53.9 ± 1.2	31.7 ± 0.4	79.8 ± 3.7
5v	36.8 ± 0.1	45.2 ± 2.7	–	36.8 ± 0.1	42.1 ± 4.5	48.6 ± 1.8	58.3 ± 3.4	28.9 ± 1.3	35.0 ± 3.3	22.8 ± 2.3	45.7 ± 3.6	42.1 ± 2.9
Azoxystrobin[b]	79.5 ± 4.9	55.8 ± 3.1	59.2 ± 1.5	72.5 ± 2.1	62.4 ± 4.1	61.4 ± 1.5	78.4 ± 1.1	73.6 ± 1.8	56.3 ± 4.1	38.9 ± 3.3	62.5 ± 2.2	86.3 ± 4.1

[a] Average of three replicates.
[b] The commercial antifungal agent.

Table 4 The EC_{50} values of some of the target compounds against *CG*, *RS*, *PL* and *CT*.

Compounds	EC_{50} (μg/mL)[a]			
	CG	*RS*	*PL*	*CT*
5i	–	–	–	16.1
5k	40.1	–	33.7	–
5q	–	–	28.4	–
5s	–	–	6.9	23.9
5t	–	–	10.1	–
5u	69.1	26.0	–	–
Azoxystrobin[b]	57.6	26.7	10.8	12.8

[a] Average of three replicates.
[b] The commercial antifungal agent.

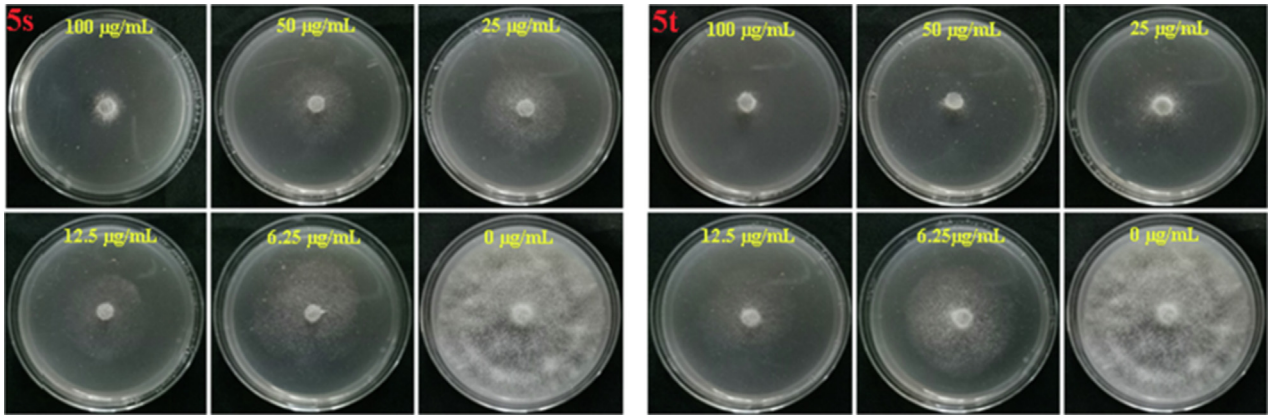

Fig. 6 Antifungal activities of compounds **5s** and **5t** against *PL in vitro*.

compounds **5h**, **5m**, **5t** and ningnanmycin to TMV-CP protein yielded K_d values of 0.499, 0.008, 69.625 and 2.338 μmol/L, respectively. As displayed in MST results that the combining capacity in the following order of **5m** > **5h** > ningnanmycin > **5t** was basically consistent with the antiviral activity, it shows that there was a good interaction between compound **5m** and TMV-CP.

*3.2.3. Molecular docking of compounds **5m** and **5t** with TMV-CP*

The molecular docking was studied that **5m** and **5t** with TMV-CP (PDB code: 1EI7) were analyzed using Discovery Studio 4.5 Client and the binding results were clearly shown in Fig. 5. Compounds **5m** and **5t** were combined with TMV-CP in one pocket respectively. Among of them, compound **5m** forms four hydrogen bonds with ARGB:261, AGRA:134, SERB:255, and LYSB:268, respectively, after docking with TMV-CP, and compound **5t** forms two hydrogen bonds with SERB:255 and ARGB:261 after docking. It can be seen that in combination with TMV-CP, compound **5m** has two more stable hydrogen bonds than that of **5t**, indicating that the antiviral activity of **5m** was better than **5t**. The interaction between these molecules and TMV-CP may weaken the interaction between the two subunits of TMV-CP, so as to prevent the self-assembly of TMV and weaken the binding ability with TMV-CP.

3.3. Antifungal activity assay

3.3.1. In vivo antifungal activity of the target compounds

The effects of the target compounds against fungal were evaluated by the mycelial growth inhibition method at 100 μg/mL. The data in Table 3 showed that some of the target compounds exhibited good antifungal activity. Among them, the inhibitory activities of compounds **5i** and **5t** against *CT* were 73.2 and 71.0%, respectively, which were similar to that of azoxystrobin (72.5%). The inhibitory activities of compounds **5k** (62.2%) and **5u** (60.0%) were similar to those of azoxystrobin (61.4%) against *CG*. Compound **5u** (88.6%) showed better activity of anti-*RS* than azoxystrobin (78.4%). It is noteworthy that most of the target compounds had good inhibitory effects against *PL*. The inhibitory rates of compounds **5i** and **5p** were 81.5 and 87.3%, respectively, close to azoxystrobin (86.3%). Compounds **5k**, **5q**, **5s** and **5t** exhibited significant activity against *PL*, with values of 90.1, 93.8, 96.3 and 96.0% respectively, which were exceeded that of azoxystrobin (86.3%). To further confirm the antifungal activity of the target compound, EC_{50} tests were performed on some compounds, and the test results were shown in Table 4. The EC_{50} values of the tested compounds were close to or better than the corresponding control azoxystrobin. It was noteworthy that EC_{50} values of compound **5k** (26.0 μg/mL) against *RS* were comparable to azoxystrobin (26.7 μg/mL), and compounds **5t** and **5s** display

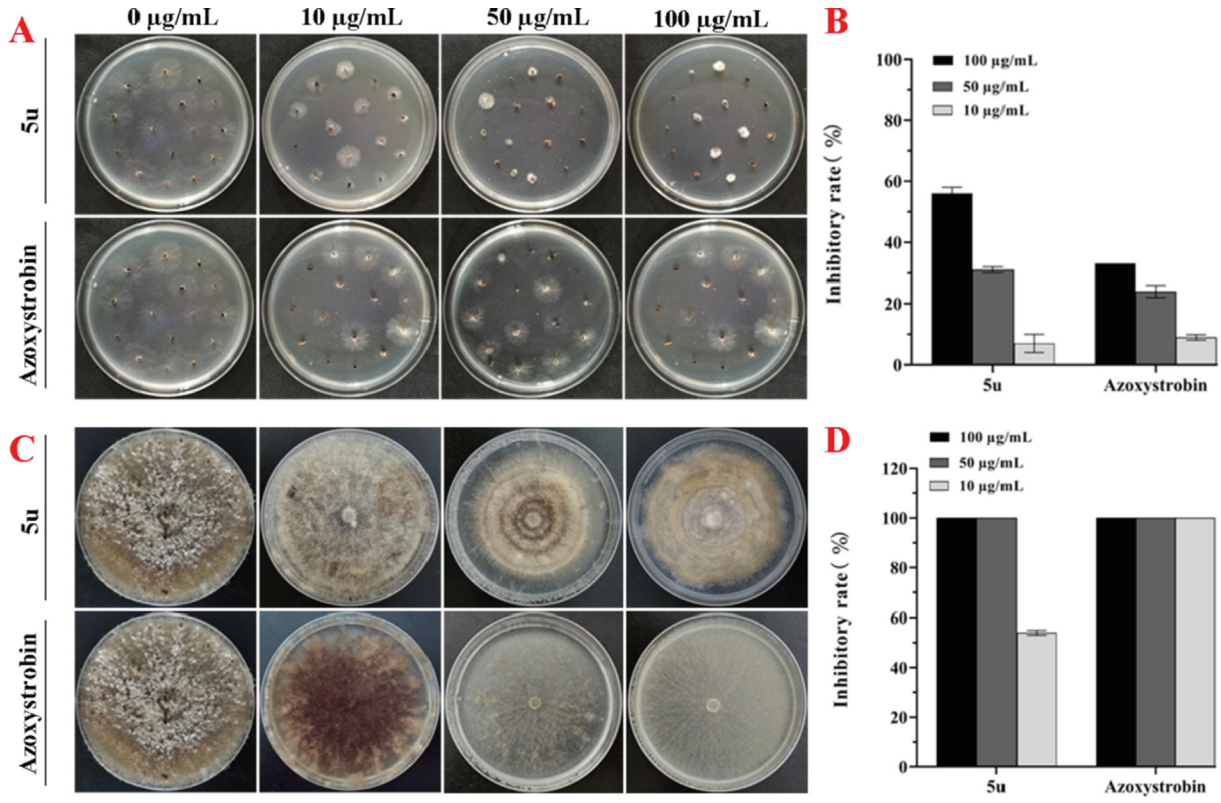

Fig. 7 Inhibitory activities of compound **5u** on sclerotia germination (A, B) and formation (C, D) of *RS*.

Table 5 The control efficacy against rice sheath blight disease of compounds **5u** on rice leaves.

Treatment	Concentration (μg/mL)	Lesion length (cm)[a]	Control efficacy (%)
5u	100	2.9 ± 0.3	55.4
	200	1.6 ± 0.2	75.4
Azoxystrobin	100	1.8 ± 0.1	72.3
	200	0.4 ± 0.4	93.8
Negative control	–	6.5 ± 0.3	–

[a] Values are the average of 15 replicates.

remarkable activity against *PL,* with EC_{50} values of 6.9 and 10.1 μg/mL (Fig. 6), respectively, which were superior compared to azoxystrobin (10.8 μg/mL).

The antifungal activity of the target compounds was also affected by different substituents on R_1 and R_2. For example, compound **5i** (R_1 = CH_3, R_2 = 6-Cl-3-Py) and **5t** (R_1 = H, R_2 = 6-Cl-3-Py) showed good inhibitory activity against *CT*, which were 73.2% and 71.0%, respectively. It is indicating that when R_2 was 6-Cl-3-Py group, the growth of *CT* could be inhibited, and when R_1 was CH_3 group could increase the anti-*CT* activity. In the anti-*RS* activity data, it can be found that CH_3, 6-Cl-3-Py, CH_2CH = CH, and 2-Cl-5-thiazoly at the R_2 group, the inhibitory activity of compounds against *RS* was mostly better than compounds with R_2 of benzyl substitution. And when R_1 was H, it helps to improve the anti-*RS* activity. Most of the target compounds had significant antifungal activities for against *PL*. For instance, when R_1 was H, compounds **5s** (R_2 = CH_3), **5t** (R_2 = 6-Cl-3-Py), **5q** (R_2 = 2-Cl-6-F-Ph) and **5p** (R_2 = 4-NO_2-Ph) were 96.3, 96.0, 93.8 and 87.3%, respectively. It is speculated that when the R_1 group was H, and the substitution activity of the R_2 group was methyl > six-membered heterocycle > benzene. When R_1 was a CH_3 group, **5i** (R_2 = 6-Cl-3-Py) and **5k** (R_2 = 2-Cl-5-thiazoly), the inhibitory activity against *PL* were 81.5% and 90.1%, respectively. When R_2 was a 2-Cl-5-thiazoly group, it could enhance the anti-*PL* activity of target compounds. Moreover, it was found that compounds **5i** and **5t** had good inhibitory activities against the above three strains, and it was inferred that the antifungal spectrum of the target compound could be improved when R_2 group was replaced by 6-Cl-3-Py.

*3.3.2. Inhibitory effect of compound **5u** on RS sclerotia germination and formation*

Fig. 7A and 7B indicated that the sclerotia germination inhibition of compound **5u** on the *RS*. Compound **5u** and azoxystrobin exhibited general inhibitory activity in a dose-dependent manner. In a word, compound **5u** showed better inhibitory effect than azoxystrobin with the inhibition of situation **5u** (100 μg/mL) > azoxystrobin (100 μg/mL) > **5u** (50 μg/mL) > azoxystrobin (50 μg/mL) > azoxystrobin (10 μg/mL) > **5u** (10 μg/mL). As shown in Fig. 7C and 7D, for treatment with compound **5u** and azoxystrobin at the concentrations of 100 and 50 μg/mL, the inhibition of sclerotia formation rate reached 100%. The inhibition rate of compound **5u** on sclerotia formation was 53.6%, but azoxystrobin was still 100%, when the treatment concentrations of 10 μg/

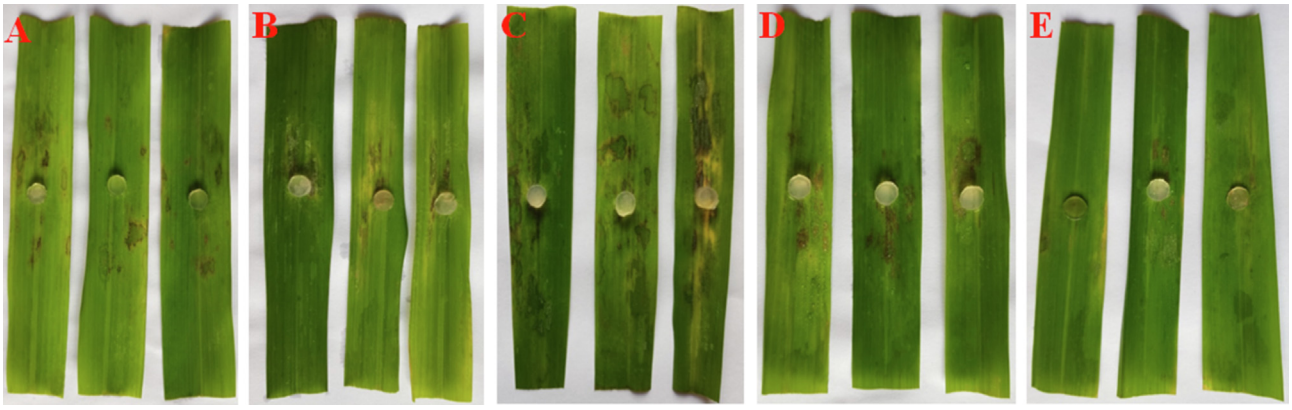

Fig. 8 The protection efficacy of compound **5u** against rice sheath blight disease on detached rice leaves. (A) **5u** at 100 μg/mL; (B) **5u** at 200 μg/mL; (C) Negative control; (D) Azoxystrobin at 100 μg/mL; (E) Azoxystrobin at 200 μg/mL.

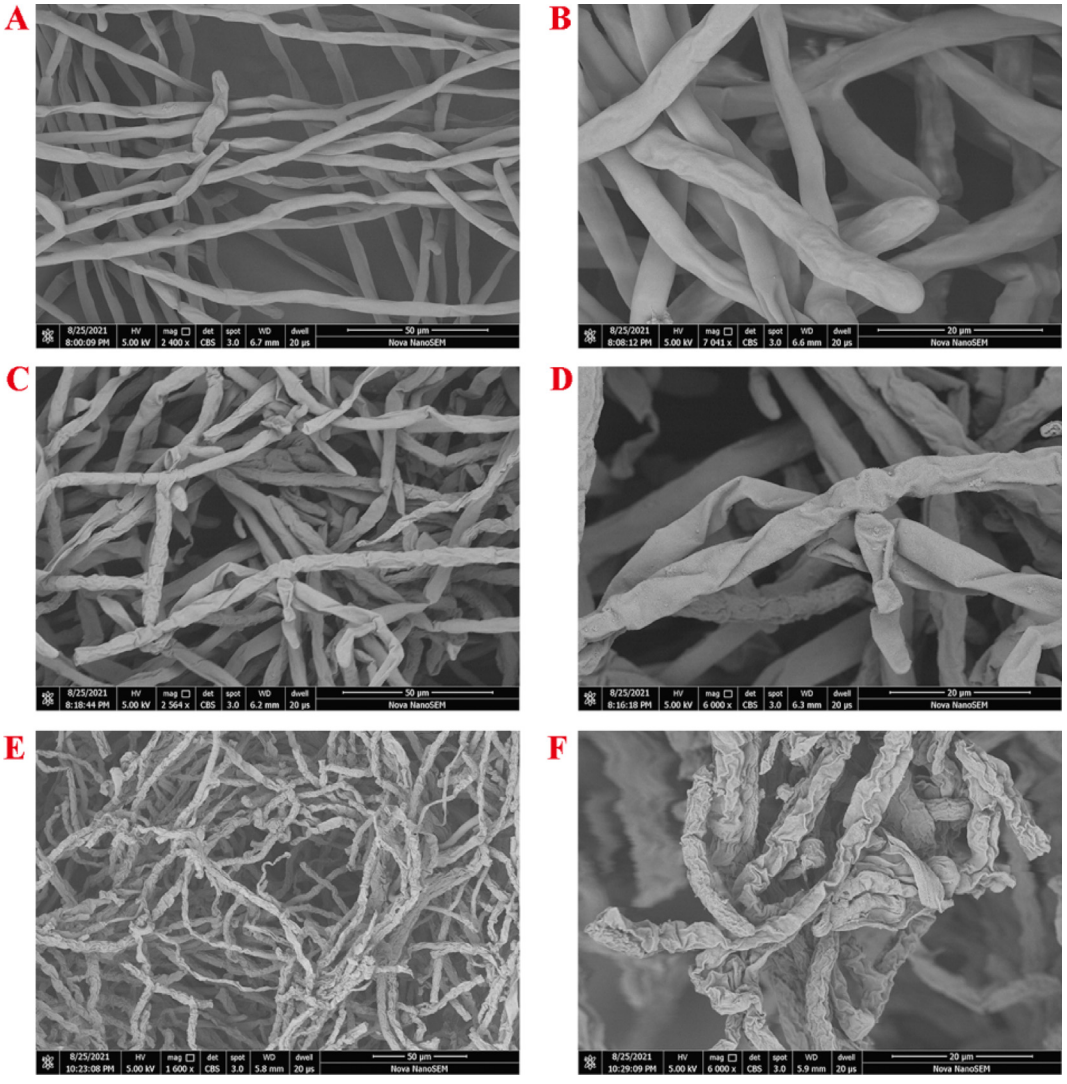

Fig. 9 Scanning electron micrographs of the hyphae of *RS* with or without compound **5u** treatment. (A, B) control groups (DMSO); (C, D) **5u** at 50 μg/mL and (E, F) **5u** at 100 μg/mL.

mL. The results indicated that compound **5u** could inhibited the sclerotia germination of *RS*. In summary, these results proved that compound **5u** could inhibit the sclerotia germination and formation of *RS*, and reduce the source infection of *RS*, so as to control the disease.

*3.3.3. The control efficacy against rice sheath blight disease of compounds **5u** on rice leaves*

In order to further understand the *in vivo* activity of compound **5u** against rice sheath blight disease, the detached leaf assay was adopted. The Table 5 and Fig. 8 showed that the control efficacies were 55.4 and 75.4%, at 100 and 200 μg/mL, respectively, which were lower than those of azoxystrobin (72.3 and 93.8%). These results indicated that compound **5u** had a certain control efficacy on rice sheath blight disease.

3.3.4. Effect of compound 5u on the hyphae morphology of RS

The effects of compound **5u** on the morphology of *RS* were observed by scanning electron microscopy (SEM). As shown in Fig. 9, the mycelium surface of untreated blank group was smooth and full, presenting a complete cylindrical shape, and good mycelium extension. In sharp contrast to the mycelium treated with compound **5u**, when the treatment was 50 μg/mL, part of the mycelium broke, and its surface shrank, folded and collapsed. When the concentration of treatment increased to 100 μg/mL, hyphae ruptured was intensified, and all hyphae showed shrinkage, collapse and distortion. It is speculated that compound **5u** might inhibited hyphae reproduction by destroying the epidermal tissue and cell membrane of *RS*.

4. Conclusion

In summary, we designed and synthesized a series of novel trifluoromethyl pyrimidine derivatives, and determined their structures by NMR, HRMS and single crystal diffraction. Bioassay results showed that some of the target compounds showed good antiviral and antifungal activities. Especially, the antiviral activity of compound **5m** was significantly better than that of ningnanmycin. The interaction mechanism between **5m** and TMV, and molecular docking were further studied, and the results were consistent with the experimental results *in vivo*. Then, the mycelial growth rate method was used to evaluate the inhibitory activity of the target compounds against 12 kinds of fungi at the treatment concentration of 100 μg/mL. The anti-*RS* activity of compound **5u** was equivalent to azoxystrobin, and its mechanism of action had been preliminarily studied. The current research had laid the foundation for the application of trifluoromethyl pyrimidine derivatives in pesticides.

Acknowledgement

The authors gratefully acknowledge the National Nature Science Foundation of China (No. 31701821), the Science Foundation of Guizhou Province (No. 20192452), Natural Science Research Project of Guizhou Education Department (No. 2018009), Frontiers Science Center for Asymmetric Synthesis and Medicinal Molecules, Department of Education, Guizhou Province (No. 2020004), Program of Introducing Talents of Discipline to Universities of China (111 Program, D20023).

Appendix A. Supplementary material

Supplementary data to this article can be found online at https://doi.org/10.1016/j.arabjc.2022.104110.

References

Alaa, Z.O., Esraa, H., Ezzat, A.H., Elsayed, H., Ahmed, A., 2022. The curative activity of some arylidene dihydropyrimidine hydrazone against Tobacco mosaic virus infestation. J. Saudi Chem. Soc. 26, 101504.

Alia, T.E., Assiria, M.A., Alzahranic, A.Y., Salem, A.M., Shatie, A. A., Alfaifie, M.Y., Elbehairi, S.E., 2021. An effective green one-pot synthesis of some novel 5-(thiophene-2-carbonyl)-6- (trifluoromethyl)pyrano[2,3-c] pyrazoles and 6-(thiophene-2-carbonyl)-7-(trifluoromethyl)pyrano[2,3-d] pyrimidines bearing chromone ring as anticancer agents. Synthetic Commun. 15, 3267–3276.

Chen, M., Wang, Y.H., Su, S.J., Chen, Y., Peng, F., Zhou, Q., Liu, T. T., Luo, H., Wang, H., Xue, W., 2020. Synthesis and biological evaluation of 1,4-pentadien-3-one derivatives containing 1,2,4-triazole. J. Saudi Chem Soc. 24, 765–776.

Chen, J., Shi, J., Yu, L., Liu, D.Y., Gan, X.H., Song, B.A., 2018. Design, synthesis, antiviral bioactivity, and defense mechanisms of novel dithioacetal derivatives bearing a strobilurin moiety. J. Agric. Food Chem. 66, 5335–5345.

Chen, Y.X., Sun, C.W., Wen, X.X., Zhang, W.G., 2013. Design, synthesis, insecticidal evaluation and molecular docking studies of cis-nitenpyram analogues bearing diglycine esters. Sci. China Chem. 56, 159–168.

Chen, M.H., Zhang, X., Luo, H.R., Zhou, Z.Y., Chen, M.H., Wu, W. N., Lu, D.W., 2022. Synthesis and antifungal and antibacterial evaluation of novel pyrimidine derivatives with glycoside scaffolds. Chem. Pap. 76, 1321–1328.

Dolsak, A., Sribar, D., Scheffler, A., Grabowski, M., Svajger, U., Gobec, S., Holze, J., Weindl, G., Wolber, G., Sova, M., 2021. Further hit optimization of 6-(trifluoromethyl)pyrimidin-2-amine based TLR8 modulators: synthesis, biological evaluation and structure-activity relationships. Eur. J. Med. Chem. 225, 113809.

Emami, L., Faghih, Z., Sakhteman, A., Rezaei, Z., Faghih, Z., Salehi, F., Khabnadideh, S., 2020. Design, synthesis, molecular simulation, and biological activities of novel quinazolinone-pyrimidine hybrid derivatives as dipeptidyl peptidase-4 inhibitors and anticancer agents. New J. Chem. 44, 19515–19531.

Guo, T., Xia, R.J., Liu, T.T., Peng, F., Tang, X.M., Zhou, Q., Luo, H., Xue, W., 2020b. Synthesis, biological activity and action mechanism study of novel chalcone derivatives containing malonate. Chem. Biodivers. 17, e2000025.

Guo, W.K., Xing, Y.J., Zhang, Q.S., Xie, J.Q., Huang, D.X., Gu, H.J., He, P., Zhou, M.R., Xu, S.F., Pang, X.F., Liu, M.Y., Yi, Z.F., Chen, Y.H., 2020a. Synthesis and biological evaluation of B-cell lymphoma 6 inhibitors of *N*-phenyl-4-pyrimidinamine derivatives bearing potent activities against tumor growth. J. Med. Chem. 63, 676–695.

Hao, Y.N., Guo, J.C., Wang, Z.W., Liu, Y.X., Li, Y.Q., Ma, D.J., Wang, Q.M., 2020. Discovery of tryptanthrins as novel antiviral and anti-phytopathogenic-fungus agents. J. Agric. Food Chem. 68, 5586–5595.

Ji, X.F., Wang, Z.W., Dong, J., Liu, Y.X., Lu, A.D., Wang, Q.M., 2016. Discovery of topsentin alkaloids and their derivatives as novel antiviral and anti-phytopathogenic fungus agents. J. Agric. Food Chem. 64, 9143–9151.

Jiang, S.C., Tang, X., Chen, M., He, J., Su, S.J., Liu, L.W., He, M., Xue, W., 2020. Design, synthesis and antibacterial activities against Xanthomonas oryzae pv. oryzae, Xanthomonas axonopodis pv. Citri and Ralstonia solanacearum of novel myricetin derivatives containing sulfonamide moiety. Pest Manag. Sci. 76, 853–860.

Liu, L.M., Wang, Z.J., Gao, C., Dai, H.L., Si, X.J., Zhang, Y., Meng, Y.Q., Zheng, J.X., Ke, Y., Liu, H.M., Zhang, Q.R., 2021b. Design, synthesis and antitumor activity evaluation of trifluoromethyl-substituted pyrimidine derivatives. Bioorg. Med. Chem. Lett. 51, 128268.

Liu, X.H., Wen, Y.H., Cheng, L., Xu, T.M., Wu, N.J., 2021a. Design, synthesis, and pesticidal activities of pyrimidin-4-amine derivatives bearing a 5-(Trifluoromethyl)-1,2,4-oxadiazole moiety. J. Agric. Food Chem. 69, 6968–6980.

Lu, A.D., Wang, J.J., Liu, T.J., Han, J., Liu, Y.H., Su, M., Chen, J.X., Zhang, H., Wang, L.Z., Wang, Q.M., 2014. Small changes result in large differences: Discovery of (-)-incrustoporin derivatives as novel antiviral and antifungal agents. J. Agric. Food Chem. 62, 8799–8807.

Luo, D.X., Guo, S.X., He, F., Chen, S.H., Dai, A.L., Zhang, R.F., Wu, J., 2020. Design, synthesis and bio-activity of α-ketoamide derivatives bearing a vanillin skeleton for crop diseases. J. Agric. Food Chem. 68, 7226–7234.

Mamdouh, A.A.Z., Galal, H.E., Nashwa, M.M., 2021. Anti-Covid-19 drug analogues: synthesis of novel pyrimidine thioglycosides as antiviral agents against SARS-COV-2 and avian influenza H5N1 viruses. ACS Omega 6, 16890–16904.

Mane, U.R., Mohanakrishnan, D., Sahal, D., Murumkar, P.R., Giridhar, R., Yadav, M., 2014. Synthesis and biological evaluation of some novel pyrido[1,2-a] pyrimidin-4-ones as antimalarial agents. Eur. J. Med. Chem. 79, 422–435.

Mohammareh, S., Shiri, D., Maleki, E., Matin, P., Beyzaei, D., Baranipour, P., Oroojalian, D., Memariani, T., 2020. Synthesis of various derivatives of [1,3]selenazolo[4,5-d] pyrimidine and exploitation of these heterocyclic systems as antibacterial, antifungal, and anticancer agents. ChemistrySelect. 5, 10060–10066.

Munikrishnappa, C.S., Suresh, G.V., Bhandare, R.R., Shaik, A.B., 2021. Design, synthesis, and biological evaluation of novel bromopyrimidine analogues as tyrosine kinase inhibitors. Arab. J. Chem. 14, 103054.

Purushothaman, B., Arumugam, P., Kulsi, G., Song, J., 2018. Design, synthesis, and biological evaluation of novel catecholopyrimidine based PDE4 inhibitor for the treatment of atopic dermatitis. Eur. J. Med. Chem. 145, 673–690.

Samata, H.A., Patil, C.V., Sarvaiya, N.J., Gulati, S.S., Patel, H.S., 2022. Synthesis, characterization and antifungal activity of novel thiazolo-pyrimidine fused heterocycles. ECS Trans. 107, 1165–1172.

Sankarganesha, M., Solomonb, R.V., Raja, J.D., 2021. Platinum complex with pyrimidine- and morpholine-based ligand: synthesis, spectroscopic, DFT, TDDFT, catalytic reduction, in vitro anticancer, antioxidant, antimicrobial, DNA binding and molecular modeling studies. J. Biomol. Struct. Dyn. 39, 1055–1067.

Seenaiah, D., Reddy, P.R., Reddy, G.M., Padmaja, A., Padmavathi, V., Krishna, N.S., 2014. Synthesis, antimicrobial and cytotoxic activities of pyrimidinyl benzoxazole, benzothiazole and benzimidazole. Eur. J. Med. Chem. 77, 1–7.

Shi, J., Luo, N., Ding, M.H., Bao, X.P., 2020. Synthesis, in vitro antibacterial and antifungal evaluation of novel 1,3,4-oxadiazole thioether derivatives bearing the 6-fluoroquinazolinylpiperidinyl moiety. Chin. Chem. Lett. 31, 434–438.

Su, S.J., Chen, M., Tang, X.M., Peng, F., Liu, T.T., Zhou, Q., Zhan, W.L., He, M., Xie, C.W., Xue, W., 2021. Design, synthesis and antibacterial activity of novel pyrimidine-containing 4*H*-chromen-4-one derivatives. Chem. Biodivers. 18, e2100186.

Tang, X., Su, S.J., Chen, M., He, J., Xia, R.J., Guo, T., Chen, Y., Zhang, C., Wang, J., Xue, W., 2019. Novel chalcone derivatives containing a 1,2,4-triazine moiety: design, synthesis, antibacterial and antiviral activities. RSC Adv. 9, 6011–6020.

Wang, S., Zhang, R., Zhang, H., Wang, Y.C., Yang, D., Zhao, Y.L., Yan, G.Y., Xu, G.B., Guan, H.Y., Zhou, Y.H., Cui, D.B., Liu, T., Li, Y.J., Liao, S.G., Zhou, M., 2021. Design, synthesis, and biological evaluation of 2,4-diamino pyrimidine derivatives as potent FAK inhibitors with anti-cancer and antiangiogenesis activities. Eur. J. Med. Chem. 222.

Wang, X.B., Fu, X.C., Yan, J.H., Wang, A., Wang, M.Q., Chen, M., Yang, C.L., Song, Y.M., 2019. Design and synthesis of novel 2-(6-thioxo-1,3,5-thiadiazinan -3-yl)-*N*′-phenylacethydrazide derivatives as potential fungicides. Mol. Divers. 23, 573–583.

Wang, B., Zhao, B., Pang, L.P., Zhao, Y.D., Guo, Q., Wang, J.W., Zheng, Y.C., Zhang, X.H., Liu, Y., Liu, G.Y., Guo, W.G., Wang, C., Li, Z.H., Mao, X.J., Yu, B., Ma, L.Y., Liu, H.M., 2017. LPE-1, an orally active pyrimidine derivative, inhibits growth and mobility of human esophageal cancers by targeting LSD1. Pharmacol. Res. 122, 66–77.

Wu, W.N., Chen, Q., Tai, A.Q., Jiang, G.Q., Ouyang, G.P., 2015. Synthesis and antiviral activity of 2-substituted methylthio-5-(4-amino-2-methylpyrimidin -5-yl)-1,3,4-oxadiazole derivatives. Bioorg. Med. Chem. Lett. 25, 2243–2246.

Wu, W.N., Chen, M.H., Wang, R., Tu, H.T., Yang, M.F., Ouyang, G.P., 2019b. Novel pyrimidine derivatives containing an amide moiety: design, synthesis, and antifungal activity. Chem. Pap. 73, 719–729.

Wu, W.N., Chen, M.H., Fei, Q., Ge, Y.H., Zhu, Y.Y., Chen, H.J., Yang, M.F., Ouyang, G.P., 2020. Synthesis and bioactivities study of novel pyridylpyrazol amide derivatives containing pyrimidine motifs. Front. Chem. 8, 522–530.

Wu, N.J., Cheng, L., Wang, J., Yu, J.P., Xing, J.H., Xu, T.M., Wei, Y.C., 2019a. Synthesis and insecticidal activity of novel 4-arylamino pyrimidine derivatives. Chin. J. Org. Chem. 39, 852–860.

Wu, W.N., Lan, W.J., Wu, C.Y., Fei, Q., 2021. Synthesis and antifungal activity of pyrimidine derivatives containing an amide moiety. Front. Chem. 9, 695628.

Yang, L.L., Li, G.B., Ma, S., Zou, C., Zhou, S., Sun, Q.Z., Cheng, C., Chen, X., Wang, L.J., Feng, S., Li, L.L., Yang, S.Y., 2013. Structure-activity relationship studies of pyrazolo[3,4-d]pyrimidine derivatives leading to the discovery of a novel multikinase inhibitor that potently inhibits FLT3 and VEGFR2 and evaluation of its activity against acute myeloid leukemia in vitro and in vivo. J. Med. Chem. 56, 1641–1655.

Yu, X.T., Lan, W.J., Chen, M.H., Xu, S., Luo, X.X., He, S.H., Chen, H.J., Fei, Q., Wu, W.N., 2021. Synthesis and antifungal and insecticidal activities of novel *N*-phenylbenzamide derivatives bearing a trifluoromethylpyrimidine moiety. J. Chem. 8370407.

Zan, N.N., Xie, D.D., Li, M., Jiang, D.H., Song, B.A., 2020. Design, synthesis, and anti-ToCV activity of novel pyrimidine derivatives bearing a dithioacetal moiety that targets ToCV coat protein. J. Agric. Food Chem. 68, 6280–8285.

Zhang, P.F., Guan, A.Y., Xia, X.L., Sun, X.F., Wei, S.Y., Yang, J.L., Wang, J.F., Li, Z.N., Lan, J., Liu, C.L., 2019. Design, synthesis, and structure-activity relationship of new arylpyrazole pyrimidine ether derivatives as fungicides. J. Agric. Food Chem. 67, 11893–11900.

Zhang, J., Peng, J.F., Bai, Y.B., Wang, P., Wang, T., Gao, J.M., Zhang, Z.T., 2016. Synthesis of pyrazolo[1,5-a]pyrimidine derivatives and their antifungal activities against phytopathogenic fungi in vitro. Mol. Divers. 20, 887–896.

Zhang, Z.J., Zeng, Y., Jiang, Z.Y., Shu, B.S., Sethuraman, V., Zhong, G.H., 2018a. Design, synthesis, fungicidal property and QSAR studies of novel *β*-carbolines containing urea, benzoylthiourea and benzoylurea for the control of rice sheath blight. Pest Manag. Sci. 74, 1736–1746.

Zhang, Z.J., Jiang, Z.Y., Zhu, Q., Zhong, G.H., 2018b. Discovery of *β*-carboline oxadiazole derivatives as fungicidal agents against rice sheath blight. J. Agric. Food Chem. 66, 9598–9607.

Zühal, K.K., Nuri, O., Filiz, B.A., 2020. Synthesis and anticancer activity of some pyrimidine derivatives with aryl urea moieties as apoptosis- inducing agents. Bioorg. Chem. 101, 104028.

Zuo, Y., Wu, Q.Y., Su, S.W., Niu, C.W., Xi, Z., Yang, G.F., 2016. Synthesis, herbicidal activity, and QSAR of novel *N*-benzothiazolylpyrimidine -2,4-diones as protoporphyrinogen oxidase inhibitors. J. Agric. Food Chem. 64, 552–562.